Taylor & Francis
Taylor & Francis Group

LABORATORY STUDY

🔓 OPEN ACCESS | Check for updates

# Sirt6 overexpression relieves ferroptosis and delays the progression of diabetic nephropathy via Nrf2/GPX4 pathway

Lingyu Du[#], Canghui Guo[#], Shengnan Zeng[#], Ke Yu[#], Maodong Liu[#] and Ying Li[#]

Department of Nephrology, Hebei Medical University Third Hospital, Shijiazhuang City, Hebei Province, China

## ABSTRACT

**Objective:** Sirt6, reactive oxygen species and ferroptosis may participate in the pathogenesis of Diabetic Nephropathy (DN). Exploring the relationship between Sirt6, oxidative stress, and ferroptosis provides new scientific ideas to DN.

**Methods:** Human podocytes were stimulated with 30 mM glucose and 5.5 mM glucose. The mice of db/db group were randomly divided into two groups:12 weeks and 16 weeks. Collect mouse blood and urine specimens and renal cortices for investigations. HE, Masson, PAS and immunohistochemical staining were used to observe pathological changes. Western blot, RT-qPCR and immunofluorescence staining were used to evaluate expression of relevant molecules. CCK8 method was introduced to observe cell viability. The changes of podocyte mitochondrial membrane potential and mitochondrial morphology in each group were determined by JC-1 staining and Mito-Tracker.

**Results:** The expression level of Sirt6, Nrf2, SLC7A11, HO1, SOD2 and GPX4 were reduced, while ACSL4 was increased in DN. Blood glucose, BUN, Scr, TG, T-CHO and 24h urine protein were upregulated, while ALB was reduced in diabetic group. The treatment of Ferrostatin-1 significantly improved these changes, which proved ferroptosis was involved in the development of DN. Overexpression of Sirt6 might ameliorate the oxidation irritable reaction and ferroptosis. Sirt6 plasmid transfection increased mitochondrial membrane potential and protected morphology and structure of mitochondria. The application of Sirt6 siRNA could aggravated the damage manifestations.

**Conclusion:** High glucose stimulation could decrease the antioxidant capacity and increase formation of ROS and lipid peroxidation. Sirt6 might alleviate HG-induced mitochondrial dysfunction, podocyte injury and ferroptosis through regulating Nrf2/GPX4 pathway.

## 1. Introduction

Diabetic nephropathy (DN) is a significant microvascular complication in individuals with diabetes and is a leading cause of renal failure. It is estimated that approximately 40% of type 2 diabetic patients and 30% of type 1 diabetic patients will eventually develop diabetic nephropathy. Once diabetic nephropathy sets in, the majority of patients will progress to end-stage renal disease (End Stage Renal Disease, ESRD), which has a 5-year survival rate of less than 20%. This places a substantial burden on both families and society [1–3]. The pathogenesis of DN is multifaceted and involves various factors such as glomerular hemodynamic disorders, oxidative stress, inflammation, fibrosis, metabolic disorders, autophagy, changes in intestinal microorganisms, genetic susceptibility, and epigenetic modifications [2, 4–9]. Research

has indicated that proteinuria in diabetic nephropathy is primarily caused by damage to podocytes [10]. Consequently, it is essential to investigate the patterns of podocyte damage in order to gain a comprehensive understanding of the pathogenesis of DN.

The kidney is an organ that contains a significant amount of nicotinamide adenine dinucleotide (Nicotinamide Adenine Dinucleotide, NAD+). Sirtuins, a class of NAD+-dependent histone deacetylase enzymes, consisting of seven enzymes, play crucial roles in various biological functions. Research has demonstrated that Sirtuins can enhance kidney damage caused by diabetes by regulating epigenetics, influencing multiple signaling pathways, and regulating mitochondrial function [11]. Consequently, Sirtuins have emerged as important targets in health research. Numerous studies have

**CONTACT** Ying Li ✉ 35500825@hebmu.edu.cn 🏢 Department of Nephrology, Hebei Medical University Third Hospital, No. 139 Ziqiang Road, Shijiazhuang City, Hebei Province 050011, China

[#]These authors contributed equally to this work.

confirmed the association between Sirt6 and the pathogenesis of DN. Sirt6 can reduce cellular oxidative stress, inflammatory response, and renal fibrosis, thereby maintaining cellular homeostasis and delaying the chronic progression of renal disease [12, 13]. Furthermore, Sirt6 protects the kidneys through the regulation of multiple signaling pathways, including AMPK [14], Notch [15], Smad3 [16].

Ferroptosis is a form of programmed cell death that relies on iron and is characterized by the accumulation of reactive oxygen species (reactive oxygen species, ROS). It was first proposed by Dixon in 2012 [17]. Unlike other forms of programmed cell death, ferroptosis exhibits distinct morphological and biological features. Morphologically, it is associated with increased density of the mitochondrial membrane, reduced mitochondrial cristae, and rupture of the mitochondrial outer membrane. Biologically, ferroptosis is characterized by iron accumulation, ROS accumulation, and lipid peroxidation. Additionally, it is characterized by reduced levels of glutathione and inhibition of glutathione peroxidase 4 [18]. Ferroptosis is closely associated with the pathophysiological processes of various diseases, including tumors, neurological diseases, kidney damage, and ischemia-reperfusion injury [18, 19]. The regulation of ferroptosis to intervene in the occurrence and progression of these diseases has become a prominent topic in etiology research. ACSL4, a key enzyme in fatty acid metabolism, may regulate ferroptosis by influencing oxidative stress pathways, given its role in cellular responses to reactive oxygen species accumulation. Wang et al. investigated the relationship between Sirt6 and ferroptosis, and found that in diabetic mice and cell models, reduced Sirt6 expression led to increased inflammatory response and ferroptosis [20]. Conversely, upregulation of Sirt6 expression improved ferroptosis and inflammatory response. The Nrf2/GPX4 pathway was identified as the mechanism through which Sirt6 regulates ferroptosis, with Sirt6 overexpression or knockout inhibiting or aggravating ferroptosis [21, 22]. However, the role of Sirt6 and ferroptosis in diabetic nephropathy has not been fully understood. Therefore, this study aims to investigate the expression of Sirt6 in DN and explore whether regulating Sirt6 can alleviate mitochondrial dysfunction, reduce oxidative stress, and mitigate ferroptosis induced by DN, ultimately improving the prognosis of DN. The findings from this research are expected to identify novel targets for the treatment of diabetic nephropathy.

## 2. Materials and methods

### 2.1. Animal experiments

Eight-week-old C57BL/6ks db/db mice (40±2.5 g, SPF, n=12) and db/m mice (20±2.5 g, SPF, n=12) (Huachuang Xinnuo biotechnology company, Jiangsu) were randomly assigned to each experimental group. The animal experiment was approved by the Ethics Committee of Hebei Medical University and conducted according to the animal ethical standards. The mice were sacrificed and the kidney tissues were obtained, stored at $-80\,°C$ for molecular analysis. Partial renal tissues were fixed in 4% paraformaldehyde for pathological analysis.

### 2.2. Biochemical testing of blood and urine

Mice were killed at 12 week-old and 16 week-old respectively. Mice were housed in metabolic cages individually. Blood and 24h urine samples were centrifuged for 20min to collect the supernatant for detecting blood glucose (Omron glucometer), BUN, Scr, TG, T-CHO, ALB and 24h urine protein (C013-1-1, C011-2-1, A110-1-1, A111-1-1, A028-2-1, C035-2-1, Nanjing, Jiancheng, China).

### 2.3. Histological and TEM observation

Samples were fixed in 4% paraformaldehyde for HE, Masson, and PAS staining to evaluate the morphological changes and others were fixed in glutaraldehyde for electron microscopy to observe ultrastructure. Immunohistochemical staining was performed to observe positive expression.

### 2.4. Cell culture

Conditionally immortalized human podocytes, which were purchased from Basic Medical Cell Center, Peking Union Medical College, Beijing, China. Podocytes were cultured in RPMI-1640 containing 10% fetal bovine serum and 1% penicillin-streptomycin at $37\,°C$ and 5% $CO_2$ incubator. Cells were randomly divided into normal glucose group (5.5mmol/L glucose, NG) and high glucose group (30mmol/L glucose, HG). The groups were cultured at various times (0,6,12,24,48 and 72h).

### 2.5. Immunofluorescence assay

Podocytes grown on cover slides were fixed with 4% formaldehyde for 30min at room temperature, permeabilized 10min with PBS containing 0.1% Triton X-100, blocked for 10% fetal calf serum for 30min at $37\,°C$. The samples were incubated with rabbit anti-Sirt6 polyclonal antibody (1:100, 13572-1-AP, Proteintech, Wuhan, China), rabbit anti-Nrf2 (1:50, 16396-1-AP, Proteintech), mouse anti-GPX4 (1:100, 67763-1-Ig, Proteintech), rabbit anti-SOD2 (1:50, 24127-1-AP, Proteintech), rabbit anti-HO1 (1:200, 10701-1-AP, Proteintech) overnight at $4\,°C$, and then incubated with goat anti-rabbit or goat anti-mouse IgG H&L secondary antibody at $37\,°C$ for 2h. Finally, cells were stained with DAPI (SouthernBiotech, USA) for 5min. Images were obtained using a laser scanning confocal microscope (LEICA, Germany).

### 2.6. Cell counting kit-8 (CCK-8) assay

Cells were inoculated into 96-well plates at a density of $10^5$ cells/well, incubated at $37\,°C$, 5% $CO_2$ incubator for 24h and exposed to various concentrations of the compounds. 10 μl

CCK-8 was added to each well and incubated at 37°C for 3h. Measure the with an enzyme marker. The OD value was measured on a microplate reader at 450 nm.

### 2.7. Podocyte staining for mitochondrial morphology and mitochondrial membrane potential

Human podocytes were cultured with different stimulation at 37°C. According to the manufacturer's instructions, mitochondrial morphology was determined by Mito-Tracker Red staining (C1049B, Beyotime, China). Mitochondrial membrane potential was evaluated by JC-1 staining (C2006, Beyotime, China). Laser scanning confocal microscope was adopted for observation. Image-J was employed to measure the red fluorescence density per area unit.

### 2.8. Transfection

To observe the role of Sirt6 overexpression, cells were seeded into 6-well plates at a density of $10^5$ cells/well. Sirt6 plasmid (Genepharma, Shanghai, China) and pcDNA3.1 were transfected into podocytes using lipofectamine 3000 (Invitrogen, USA) according to the manufacturer's instructions. Cells were transfected with Sirt6 siRNA (Hanheng Biotechnology, Shanghai, China) and scrambled siRNA using RNA Fit (Hanheng Biotechnology, Shanghai, China) according to the manufacturer's instructions.

The siRNA sequences were as follows:

Sirt6 siRNA sense: 5'-GAAUGUGCCAAGUGUAAGATT-3'.

Anti-sense:5'-UCUUACACUUGGCACAUUCTT-3'.

### 2.9. Western blotting

Renal tissues and cells were lysed by RIPA lysis buffer (Solarbio, Beijing, China), and then were centrifuged at 12000 rpm for 30 min at 4°C to collect the supernatant. Protease inhibitors were added to extract total protein. Equal amounts of protein samples were separated by SDS-PAGE and then transferred to polyvinylidene difluoride membranes. After blocking in 5% skimmed milk at 37°C for 1h, the PVDF membranes were incubated with primary antibodies overnight at 4°C(Sirt6 rabbit monoclonal antibody, Ab-191385, 1:1000, Abcam; Nrf2 rabbit polyclonal antibody, 1:6000, 16396-1-AP, Proteintech, Wuhan, China; HO-1 rabbit polyclonal antibody, 1:2000, 10701-1-AP, Proteintech; GPX4 rabbit polyclonal antibody, 1:1000, 30388-1-AP, Proteintech; SOD2 rabbit polyclonal antibody, 1:10000, 24127-1-AP; SLC7A11 rabbit polyclonal antibody, 1:1000, 26864-1-AP, Proteintech; ACSL4 rabbit polyclonal antibody, 1: 6000, 22401-1-AP, Proteintech; GAPDH rabbit monoclonal antibody, 1:10000, Ab-128915, Abcam;α-tubulin rabbit polyclonal antibody, 1: 10000, 66031-1-Ig, Proteintech). PVDF membranes were incubated with goat anti-rabbit/anti-mouse IgG antibody for 1h at 37°C. The membranes were treated with ECL kit ((NCM Biotech, China) and then exposed to Tanon-4800 Multi (Shanghai, China) to detect the presence of protein bands. Image-J was performed to calculate the relative expression of proteins using GAPDH or α-tubulin as the internal reference gene.

### 2.10. Quantitative real-time qPCR (RT-qPCR)

RNA was extracted using the binding column method (Omega, Total RNA Kit II)and reverse transcribed into cDNA (MonScriptTM RTIII All-in-One Mix, MR05101). cDNA was amplified with SYBR Green fluorescence PCR kit (MonAmpTM ChemoHS qPCR MIX, MQ00401). The relative amount of the target genes was standardized against GAPDH/β-actin and analyzed using the $2^{-\Delta\Delta CT}$ method.

PCR primers were as follows:

| Primer name | Sequence (5'-3') |
| --- | --- |
| Mouse Sirt6-Forward | CGGCTACGTGGATGAGGTGATG |
| Mouse Sirt6-Reverse | GAGGTGGCAGGGCTTTGTCTAG |
| Human Sirt6-Forward | AATTACGCGGCGGGGCT |
| Human Sirt6-Reverse | CGCGCGCTCTCAAAGGT |
| Mouse Nrf2-Forward | GTTGCCACCGCCAGGACTAC |
| Mouse Nrf2-Reverse | AAACTTGTACCGCCTCGTCTGG |
| Human Nrf2-Forward | ACGGTATGCAACAGGACATTGAGC |
| Human Nrf2-Reverse | TGTGGAGAGGATGCTGCTGAAGG |
| Mouse GPX4-Forward | CTCCGAGTTCCTGGGCTTGTG |
| Mouse GPX4-Reverse | CCGTCGATGTCCTTGGCTGAG |
| Human GPX4-Forward | GGCTTCGTGTGCATCGTCACC |
| Human GPX4-Reverse | TTCACCACGCAGCCGTTCTTG |
| Mouse β-actin-Forward | AGAGGGAAATCGTGCGTGAC |
| Mouse β-actin-Reverse | CAATAGTGATGACCTGGCCGT |
| Human GAPDH-Forward | TCAACAGCGACACCCACTCC |
| Human GAPDH-Reverse | TGAGGTCCACCACCCTGTTG |

Primers used in real-time PCR.

### 2.11. GSH, MDA and Mn-SOD assay

Kidney tissues and cells were collected after centrifugation. GSH, MDA and SOD were measured by GSH, MDA and SOD Assay Kit (A006-2-1, A003-4-1, A001-3, Nanjing, Jiancheng, China). The OD value was measured on a microplate reader.

### 2.12. Statistical analysis

Statistical analysis was performed using Prism 10.0 software (GraphPad, USA). All values were presented as the mean±SD. For two group comparison, t-test was presented. For multiple group comparison, one-way ANOVA analysis was presented. $p < 0.05$ was defined as statistically significance. All studies were repeated times under the same experimental condition.

## 3. Result

### 3.1. General conditions and changes in biochemical indicators of diabetic nephropathy mice

The body weight of mice in the diabetic nephropathy db/db group was significantly higher than that of the control db/m group at both 12 weeks and 16 weeks of age. The kidney/body weight of the db/db group was lighter than that of the db/m group at the same age ($p < 0.05$). Additionally, the db/db group exhibited higher levels of blood sugar, blood creatinine, urea nitrogen, 24-h urine protein quantification, blood cholesterol, and blood triglycerides compared to the

db/m group ($p < 0.05$). Conversely, blood albumin levels were lower in the db/db group compared to the db/m group, indicating a decrease ($p < 0.05$) (Figure 1, Table 1).

## 3.2. Morphological changes in the kidneys of mice with diabetic nephropathy

Morphological staining did not reveal any obvious abnormalities in the renal tissues of the db/m group. However, compared to the db/m group, HE staining showed an increase in glomerular volume and compensatory hypertrophy of some renal tubules. There was also infiltration of inflammatory cells in the renal interstitium. Masson staining revealed diffuse or irregular thickening of the glomerular basement membrane and an increase in extracellular matrix. Additionally, PAS staining showed that in the db/db group, the glomeruli were enlarged, some renal tubular epithelial cells were degenerated and atrophied, the capillary basement membrane was diffusely thickened, and the mesangial matrix increased. Electron microscopy showed extensive fusion of foot processes and irregular thickening of the basement membrane (Figure 2).

## 3.3. Expression of Sirt6, oxidative stress, and ferroptosis proteins in renal tissue of diabetic mice

The expression of Sirt6, Nrf2, ACSL4, HO1, SOD2, and GPX4 was detected in the kidneys of the db/m group and db/db group.

Western blot results showed a significant reduction in the protein expressions of Sirt6, Nrf2, HO1, SOD2, and GPX4 in the kidneys of mice in the db group compared to the db/m group, while the expression of ACSL4 protein was significantly increased (Figure 3A, 3B). Real-time qPCR analysis also confirmed a significant reduction in the mRNA expression of Sirt6, Nrf2, and GPX4 in the kidneys of mice in the db/db group compared to the db/m group, consistent with the Western blot results (Figure 3C). Immunohistochemical staining further demonstrated a significant reduction in the expression of Sirt6 in the db/db group compared to the db/m group (Figure 3D). Immunofluorescence experimental results show that the expression of Sirt6 in podocytes from diabetic db/db mouse model group is significantly lower than that in the control db/m mouse group, WT-1 was used as podocyte marker (Figure 3E).

## 3.4. Expression of Sirt6, oxidative stress, and ferroptosis proteins in glomerular podocytes was investigated

The expression of Sirt6, oxidative stress, and ferroptosis protein was detected in human glomerular podocytes cultured with high glucose. Western blot and Real-time qPCR were used to measure the protein expression and mRNA levels, respectively. The results showed that Sirt6 protein expression increased after 6h of high glucose stimulation, reached a peak at 12h, began to decrease at 24h, and then inclined to a minimum at 48h. The expression of ACSL4 protein increased after
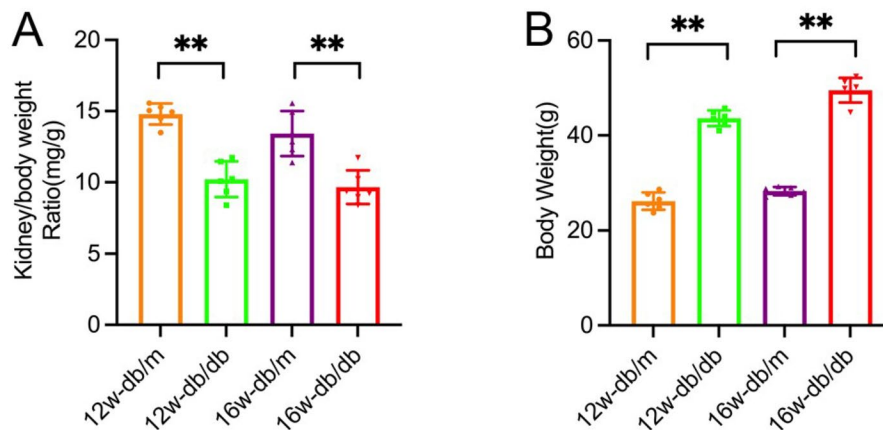


Figure 1. Body weight and kidney/body weight of db/m group and db/db group at various ages. Data are presented as mean ± SD; db/m: normal control group; db/db: diabetic group; $n = 6$; *$p < 0.05$, **$p < 0.01$ db/db vs db/m.

Table 1. BUN、Scr、24h urinary protein、blood glucose、ALB、TG、T-CHO in db/m group and db/db group at 12,16 weeks. *$p < 0.05$, **$p < 0.01$ db/db vs db/m.

| week | group | BUN (mmol/L) | Scr (mmol/L) | UP (mg/24h) | Blood Glucose (mmol/L) |
|------|-------|--------------|--------------|-------------|------------------------|
| 12w | db/m | 8.87 ± 0.90 | 12.48 ± 0.56 | 0.94 ± 0.11 | 8.97 ± 0.38 |
|  | db/db | 12.17 ± 0.38** | 21.95 ± 1.39** | 3.20 ± 0.44** | 29.96 ± 0.98** |
| 16w | db/m | 7.22 ± 0.14 | 11.3 ± 0.41 | 0.78 ± 0.07 | 8.97 ± 0.38 |
|  | db/db | 13.55 ± 0.95** | 23.95 ± 1.34** | 4.58 ± 0.16** | 31.23 ± 1.37** |

| week | group | ALB (g/L) | TG (mmol/L) | T-CHO (mmol/L) |
|------|-------|-----------|-------------|----------------|
| 12w | db/m | 30.1 ± 0.53 | 0.6 ± 0.11 | 1.88 ± 0.11 |
|  | db/db | 25.67 ± 1.02** | 1.06 ± 0.12 | 2.67 ± 0.05** |
| 16w | db/m | 27.97 ± 0.58 | 1.01 ± 0.12 | 2.31 ± 0.19 |
|  | db/db | 21.13 ± 2.61** | 5.06 ± 0.46** | 3.04 ± 0.13** |
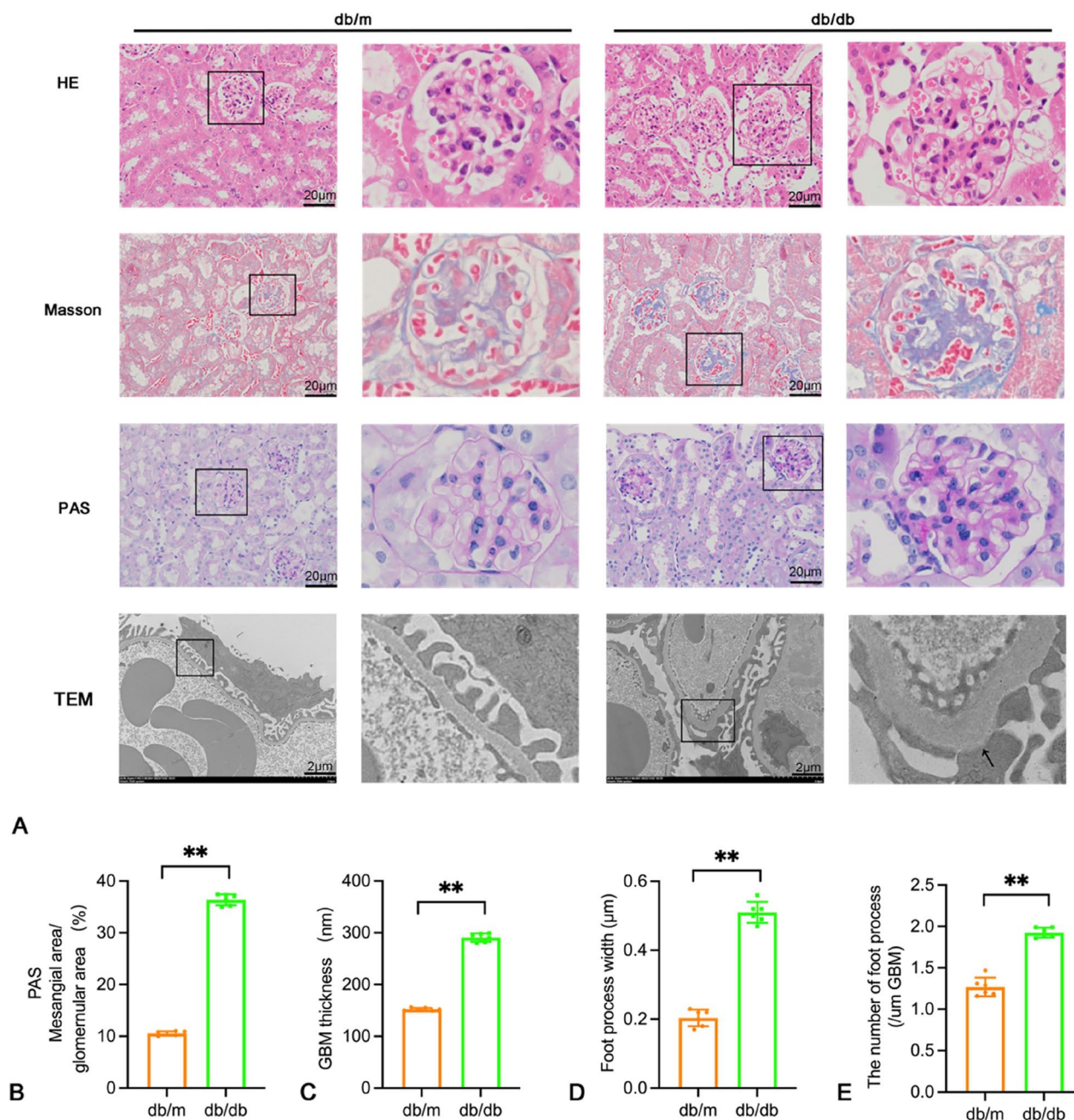
**Figure 2.** Pathological and ultrastructural changes in the kidneys of the mouse control group and the 16-week diabetic group. (A) HE, masson, PAS staining (×400, scale bar = 20 um) and electron micrographs in renal tissues of db/m group and db/db group. TEM scale bar = 2 um. (B–E) The mesangial area/glomemular area, GBM thickness, foot process width and the number of foot process (/um GBM) were shown using a histogram. Data are presented as mean±SD; db/m: normal control group; db/db: diabetic group; *$p < 0.05$, **$p < 0.01$ db/db vs db/m.

6h and peaked at 48h. Nrf2 protein reached its lowest level at 48h after high glucose stimulation. SLC7A11 and GPX4 proteins decreased to a minimum at 24h. The expression of HO1 protein began to increase with high glucose stimulation at 6h and started to decline at 24h. SOD2 started to decrease at 48h. The mRNA levels of Sirt6 were consistent with the Western blot results, increasing at 6h and then incling to a minimum at 48h, which was statistically significant. The mRNA levels of Nrf2 reached its lowest points at 48h after high glucose stimulation, with GPX4 mRNA also decreasing at 24h. The aim was to detect the expression and localization of Sirt6 in glomerular podocytes under high glucose stimulation. The time point with the lowest expression of Sirt6 in glomerular podocytes under high glucose stimulation was selected. At 48h, cell immunofluorescence staining revealed a significant reduction in the expression of Sirt6 in the HG group compared to the normal group (green fluorescence), with predominant expression in the nucleus. Nrf2 and SOD2 were stimulated with high glucose for 48h, while HO1 and GPX4 were stimulated for 24h. Cell immunofluorescence staining showed reduced expression of the HG group compared to the normal group (Figure 4).
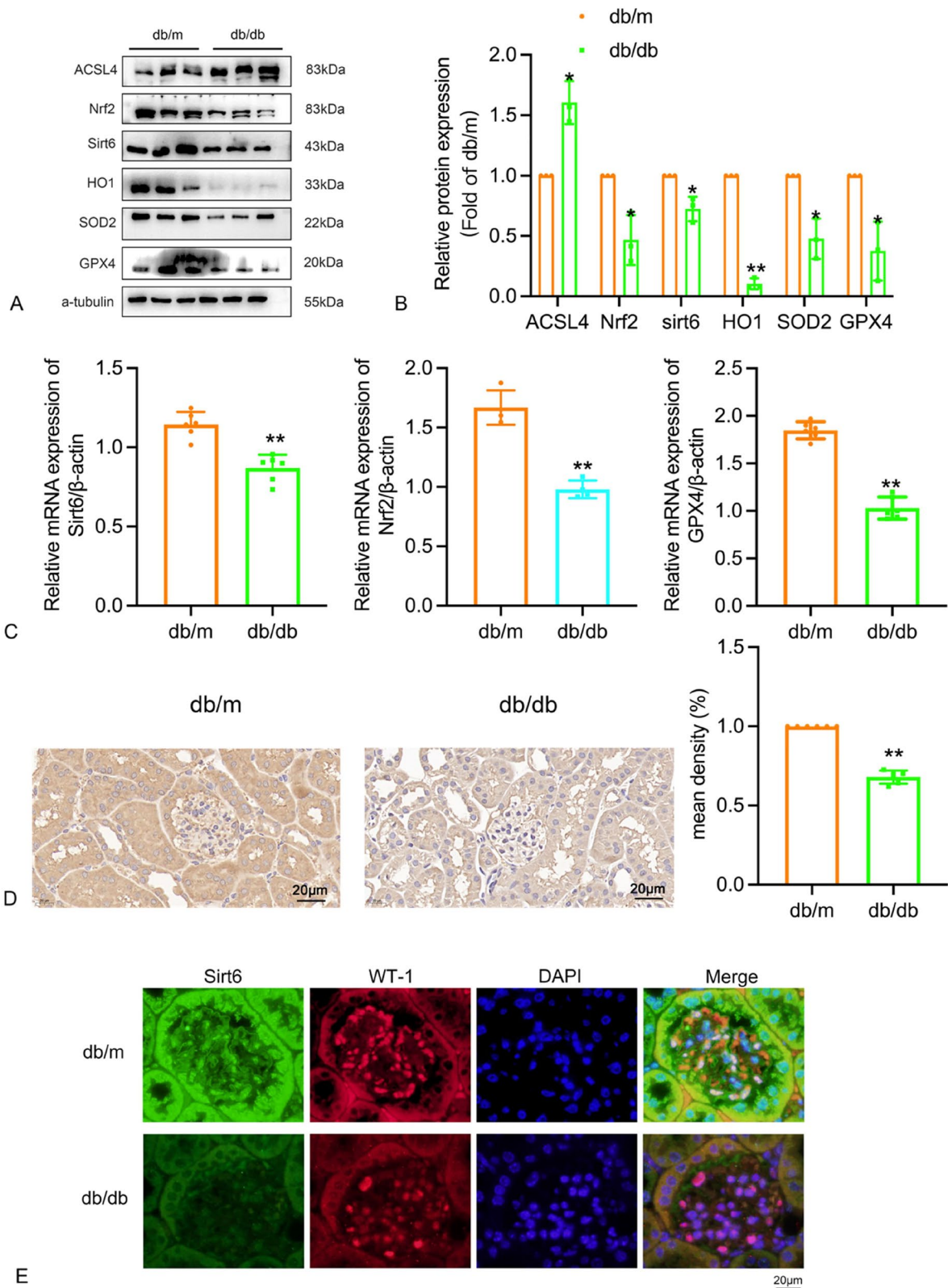
**Figure 3.** Expression of Sirt6 in renal tissues of db/m and db/db 16w group. (A–B) The proteins level of Sirt6, ACSL4, Nrf2, HO1, SOD2 and GPX4 were analyzed by Western blot in renal tissue of db/m and db/db group and shown using a histogram. (C)The mRNA levels of Sirt6, Nrf2, GPX4 were determined by real-time qPCR in renal tissues of db/m group and db/db group and shown using a histogram. (D) Immunohistochemical staining for Sitr6 in renal tissue of db/m group and db/db group. (E) The expression of Sirt6 in podocytes from db/db mice and db/m mice by immunofluorescence, WT-1 was used as podocyte marker. db/m: normal control group; db/db: 16w diabetic group; *$p < 0.05$, **$p < 0.01$ db/db vs db/m.

## 3.5. Effect of Fer-1 on oxidative stress and ferroptosis in podocytes induced by high glucose

### 3.5.1. Measurement of cell viability after administering different concentrations of Fer-1

To determine the optimal concentration of Fer-1, various concentrations of Fer-1 (0, 0.1, 1, 10, 20, 50, 70, 100uM) were administered and the cell viability of each group was measured. In the NG group, giving 0.1, 1, and 10uM Fer-1 significantly increased HPC cell activity compared to the 0uM control group ($p < 0.05$). However, at concentrations of 20, 50, 70, and 100uM, Fer-1 significantly inhibited HPC cell activity.

Similar conclusions were drawn in the high-glucose culture group ($p < 0.05$, Figure 5A). Therefore, a concentration of 10uM Fer-1 was selected for experimental studies.

### 3.5.2. Ferroptosis observed in HPC cultured with high glucose

To confirm the presence of ferroptosis in the glomerular podocyte model induced by high glucose, we conducted an experiment using the ferroptosis inhibitor Ferrostatin-1 (Fer-1, 10uM) to investigate its effect (Figure 5A). The cells were divided into four groups: NG group, NG + Fer-1 group, HG group, and HG + Fer-1 group. Western blot analysis was
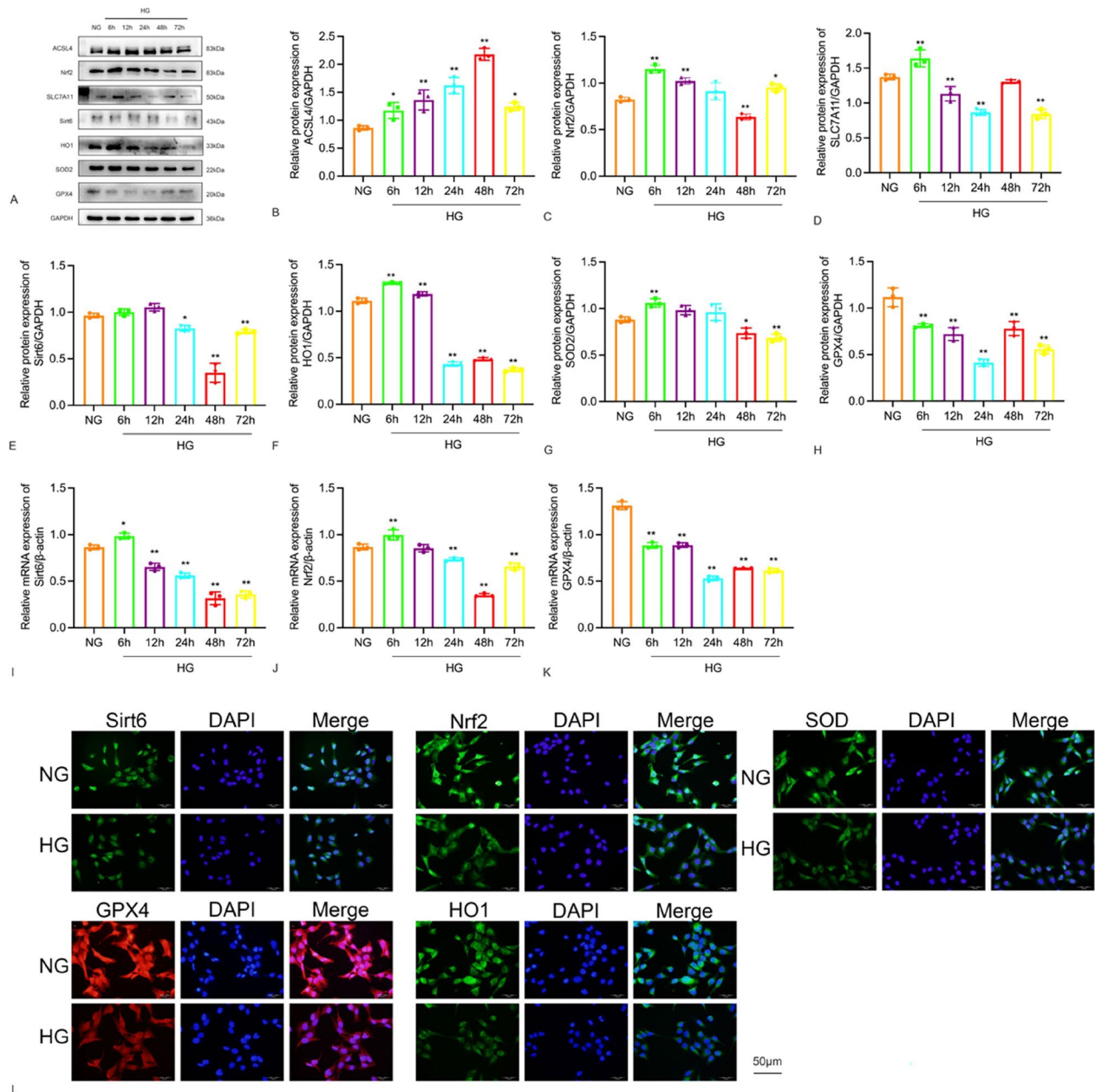


**Figure 4.** Expression of Sirt6, Nrf2, GPX4, HO1 and SOD2 in HPC cells after stimulation with 30 mM D-glucose at various time points. (A–H) The protein levels were analyzed by Western blot and shown using a histogram. (I–K) The mRNA levels of Sirt6, Nrf2, GPX4 were determined by quantitative real-time PCR in HPC cells after stimulation with 30 mM D-glucose at various time points and shown using a histogram. (L) Immunofluorescence for Sirt6, Nrf2, GPX4, HO1, SOD2 in HPC cells in NG and HG (×400). *$p < 0.05$, **$p < 0.01$.

performed to assess the expression of ferroptosis-related markers ACSL4, Nrf2, SLC7A11, and GPX4. Western blot was used to detect the expression of ferroptosis-related indicators, including ACSL4, Nrf2, SLC7A11, and GPX4. The results showed that compared with the NG group, the expression of Nrf2, SLC7A11, and GPX4 was increased, while the expression of ACSL4 was decreased in the NG + Fer-1 group. Similarly, when compared to the HG group, the HG + Fer-1 group exhibited increased expression of Nrf2, SLC7A11, and GPX4, and decreased expression of ACSL4 ($p < 0.05$). The results demonstrated that high glucose induces ferroptosis in the podocyte injury model, and the use of Fer-1 can reduce the incidence of ferroptosis (Figure 5B).

### 3.5.3. Ferroptosis inhibitor Fer-1 reduces lipid peroxidation induced by high glucose and plays a protective role for podocyte mitochondria

To further validate our previous conclusion regarding the presence of ferroptosis and the impact of Fer-1 on lipid peroxidation, we divided the cells into three groups: NG group, HG group, and HG + Fer-1 group. We employed GSH, MDA, and SOD kits to measure intracellular levels of GSH, MDA, and SOD in each group (Figure 5C). The results showed that compared to the NG group, the HG group exhibited decreased expression of GSH and SOD, and increased expression of MDA. However, the HG + Fer-1 group demonstrated

increased expression of GSH and SOD, and decreased expression of MDA when compared to the HG group.

Mito tracker was used to observe changes in mitochondrial morphology across various groups of cells. As shown in Figure 5D, compared to the mitochondria in the NG group, the mitochondria in the HG group exhibited punctate fragmentation, suggesting that the structural integrity of the mitochondria was compromised. The intervention with Fer-1 significantly improved the mitochondrial structural damage caused by high glucose stimulation (Figure 5E). This confirms that Fer-1 can ameliorate mitochondrial damage in podocytes induced by high glucose. These findings indicate that Fer-1 can protect against podocyte damage caused by high glucose, thereby reducing podocyte damage.

### 3.6. Effects of transfection of Sirt6 plasmid and Sirt6 siRNA on mitochondrial dysfunction and ferroptosis in podocytes under high glucose environment

To further investigate the impact of Sirt6 on oxidative stress, mitochondrial morphology, and function in podocytes induced by high glucose, the podocytes were divided into several groups: NG group, HG group, HG + pcDNA3.1, HG + pcDNA3.1 Sirt6, HG + Scrambled siRNA, and HG + Sirt6 siRNA. Western blot analysis was performed to measure the expression of ferroptosis-related proteins (Nrf2, ACSL4, GPX4) and oxidative stress-related protein (HO1). Cell mitochondrial
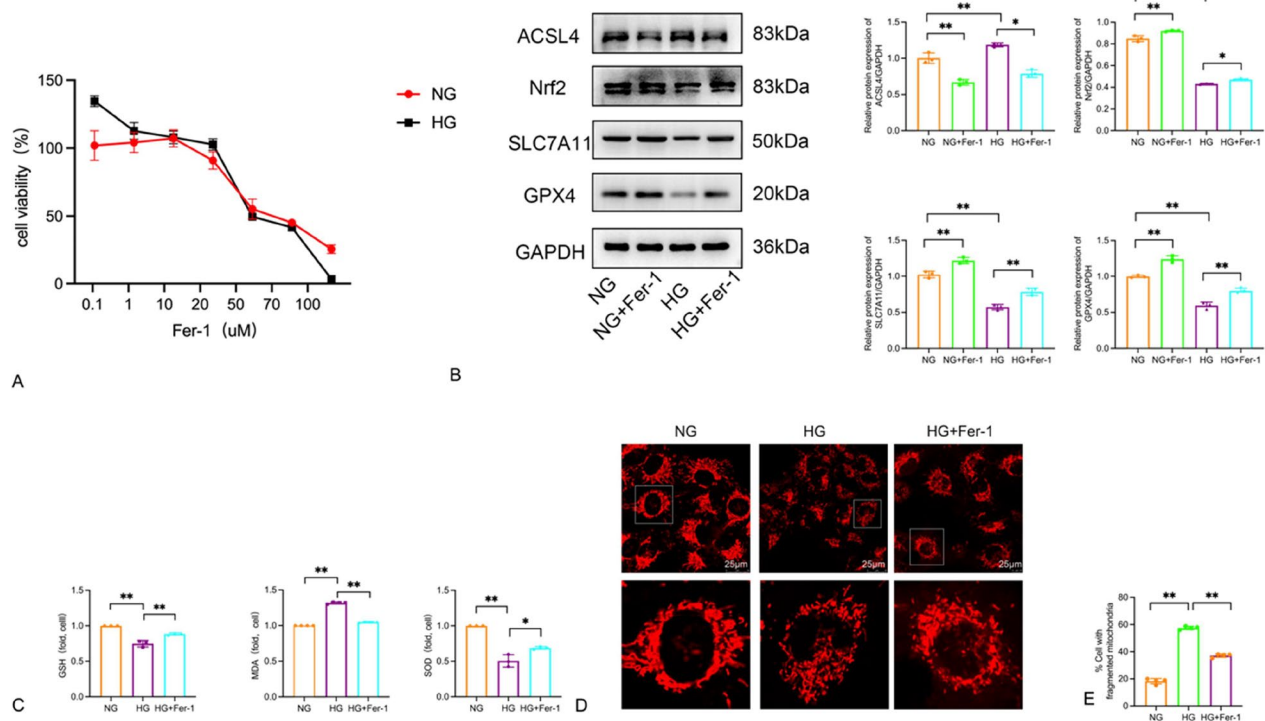


**Figure 5.** High glucose-induced ferroptosis and mitochondrial alterations in HPC cells: Effects of Fer-1. (A) The viability of HPC cells being cultured in 30 mmol/L glucose medium with different concentrations of Fer-1 for 48 h. (B) Protein blots and quantitative analysis of ACSL4, Nrf2, SLC7A11 and GPX4. (C) High glucose triggered ferroptosis-related changes in HPC cells. The GSH, MDA and SOD concentrations in cells. Data are expressed as mean ± SD. (D–E) Morphology of mitochondria and mitochondrial fragmentation in HPC cells induced by high glucose after the ferroptosis inhibitor Ferrostatin-1 intervention were detected by mito tracker red probe. *$p < 0.05$, **$p < 0.01$.

membrane potential and mitochondrial morphology were assessed using JC-1 and Mito tracker.

As shown in Figure 6A–F, the Western blot results indicated that the HG + pcDNA3.1 Sirt6 group effectively reversed the downregulation of Sirt6, Nrf2, GPX4, and HO1 compared to the HG group. Furthermore, the HG + Sirt6 siRNA group exhibited a more pronounced decrease in Sirt6, Nrf2, GPX4, and HO1 compared to the HG group. In this study, we compared the HG + pcDNA3.1 Sirt6 group and the HG + Sirt6 siRNA group with the HG group, as shown in Figure 6G–1. The mitochondrial membrane potential of the HG + Sirt6 siRNA group was found to be lower than that of the HG group. On the other hand, the HG + pcDNA3.1 Sirt6 group showed an increase in mitochondrial membrane potential compared to the HG group. However, it is important to note that the mitochondrial membrane potential of all high-glucose stimulation groups remained lower than that of the NG group ($p < 0.05$, indicating statistical significance). Moving on to Figure 6J, the confocal microscope images obtained using the Mito tracker red probe revealed distinct differences in mitochondrial morphology between the NG group and the HG group. The mitochondria in the NG group appeared filamentous, while those in the HG group were shorter, rod-shaped, and exhibited signs of swelling and fragmentation. Interestingly, the HG + pcDNA3.1 Sirt6 group showed less fragmentation and a higher proportion of normal morphological mitochondria compared to the HG group and HG + pcDNA3.1 group. Conversely, the HG + Sirt6 siRNA group exhibited a higher degree of mitochondrial fragmentation and a lower proportion of mitochondria with normal morphology compared to both the HG group and the HG + Scrambled siRNA group. Overall, our findings suggest that Sirt6 overexpression can effectively alleviate high glucose-induced oxidative stress and

ferroptosis in podocytes, leading to an improvement in mitochondrial dysfunction.

### 3.7. Inhibiting the Nrf2/GPX4 signaling pathway can attenuate the protective effect of Sirt6 on HPC cells stimulated with HG

#### 3.7.1. Detection of Sirt6 plasmid transfection efficiency

To enhance the transfection efficiency, Sirt6 transfection was conducted with varying reagent concentrations and plasmid amounts. The Western blot results are shown in Figure 7 Compared to the NG group, the group treated with Lipofectamine 3000 2.5 μl + pcDNA3.1 Sirt6 2 μg + P3000 4 μl exhibited a statistically significant decrease in Sirt6 protein expression levels after transfection ($p < 0.01$). In contrast, compared to the NG group, both the Lipofectamine 3000 3.5 μl + pcDNA3.1 Sirt6 2 μg + P3000 4 μl group and the Lipofectamine 3000 3.5 μl + pcDNA3.1 Sirt6 4 μg + P3000 4 μl group showed an increase in Sirt6 protein expression levels post-transfection, with the Lipofectamine 3000 3.5 μl + pcDNA3.1 Sirt6 4 μg + P3000 4 μl group demonstrating a more pronounced increase in Sirt6 protein expression, which was also statistically significant ($p < 0.01$). Therefore, the transfection concentration of Lipofectamine 3000 3.5 μl + pcDNA3.1 Sirt6 4 μg + P3000 4 μl was selected (Figure 7A–B).

#### 3.7.2. Sirt6 protects podocytes from high-glucose-induced oxidative stress and ferroptosis via the Nrf2/GPX4 pathway

To further observe whether the Nrf2/GPX4 signaling pathway is involved in the protective role of Sirt6 on podocytes under high-glucose conditions, the specific Nrf2 inhibitor ML385 was used to suppress the expression of Nrf2. The podocytes
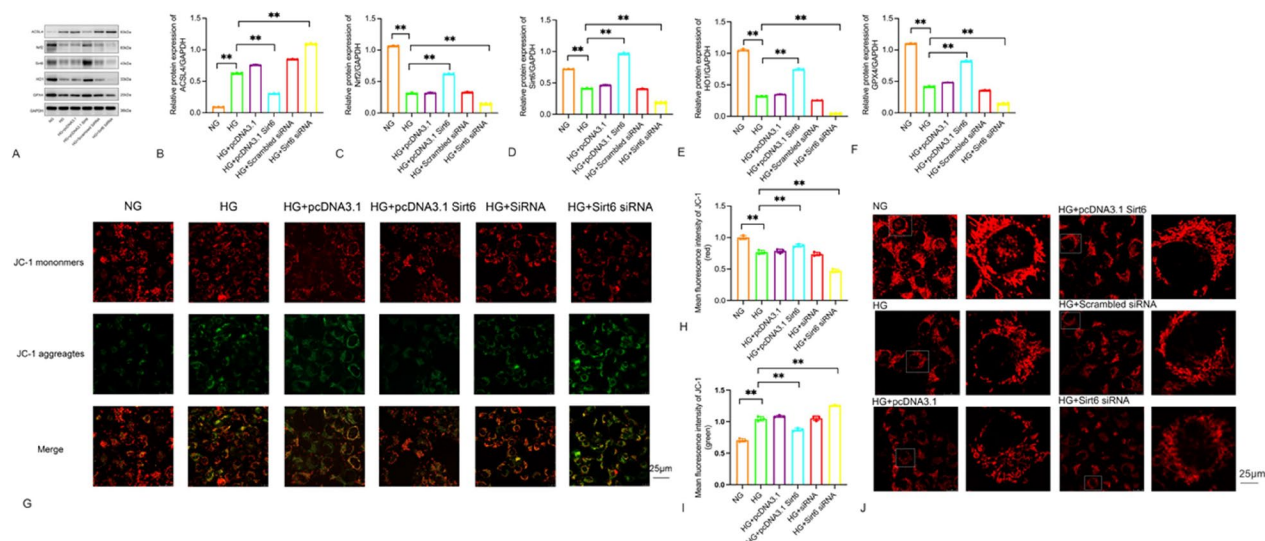


**Figure 6.** Sirt6 overexpression attenuated HG induced oxidative stress, mitochondrial dysfunction, ferroptosis and podocyte injury. (A–F) Podocytes were transfected with pcDNA3.1, pcDNA3.1 Sirt6, Scrambled siRNA, Sirt6 siRNA and then stimulated with HG (30 mM) for 48h. Western blots and quantitative analysis showing the relative protein level of Sirt6 after pcDNA3.1 Sirt6 and Sirt6 siRNA transfection of podocytes in different groups. (G–I) Membrane potential of mitochondrial in HPC cells were detected by JC-1 probe. (J) Morphology of mitochondria in HPC cells were detected by mito tracker red probe. *$p < 0.05$, **$p < 0.01$ vs NG.
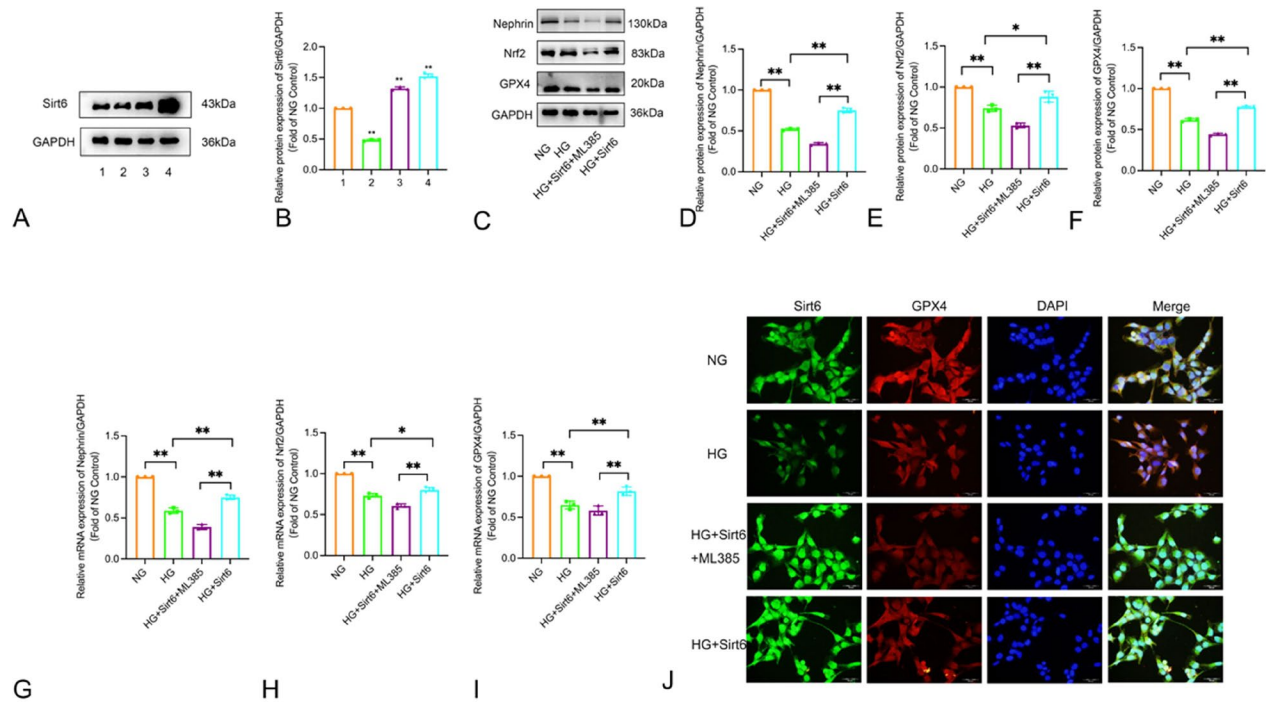
**Figure 7.** Regulation of Sirt6 expression and analysis of Nrf2, GPX4, Nephrin in HPC cells. (A)The protein levels of Sirt6 in different transfection conditions detected by Western blot. 1.NG; 2. Lipofectamin 3000 2.5 µl + pcDNA3.1 Sirt6 2 µg + P3000 4 µl; 3. Lipofectamin 3000 3.5 µl + pcDNA3.1 Sirt6 2 µg + P3000 4 µl; 4. Lipofectamin 3000 3.5 µl + pcDNA3.1 Sirt6 4 µg + P3000 4 µl. *$p < 0.05$, **$p < 0.01$ vs NG. (B–I) The expression of Nrf2, GPX4 and Nephrin in HPC cells detected by Western blot and PCR. (J) Double immunofluorescence staining of Sirt6 (green) and GPX4 (red) in HPC cells (×400). NG: normal glucose; HG: high glucose; HG + Sirt6 + ML385: HG + pcDNA3.1 Sirt6 + ML385 (5 µM); HG + Sirt6: HG + pcDNA3.1 Sirt6. *$p < 0.05$, **$p < 0.01$.

were divided into several groups: NG (5.5 mM D-glucose), HG (30 mM D-glucose), HG + pcDNA3.1 Sirt6 + ML385, HG + pcDNA3.1 Sirt6. Western blot and Real-time PCR analysis were performed to measure the expression of Nephrin, Nrf2, and GPX4. The method of cellular immunofluorescence co-staining was employed to observe the co-localization of Sirt6 and GPX4.

When compared to the HG group, overexpression of Sirt6 in a high-glucose environment can lead to an increase in the expression of the podocyte-specific protein Nephrin, indicating a protective effect on podocytes. After intervention with ML385, as shown in Figures 3–7C–I Western blot results, compared with the HG + Sirt6 group, the enhancing effect of overexpressed Sirt6 on the protein expression of Nephrin, Nrf2 and GPX in the HG + Sirt6 + ML385 group was diminished ($p < 0.05$). This suggests that after blocking Nrf2, the protective effect of overexpressed Sirt6 in reducing oxidative stress and ferroptosis in podocytes was significantly inhibited. The results of mRNA detection by real-time qPCR were consistent with the trend of Western blot ($p < 0.05$). As shown in Figures 3–7J immunofluorescence co-staining result, compared to the normal glucose (NG) group, the high glucose (HG) group showed a significant decrease in the positive expression of both Sirt6 and GPX4. Overexpression of Sirt6 could partially alleviate the reduction in GPX4 expression caused by high glucose stimulation, but the expression of GPX4 remained lower than that of the NG group. After the addition of ML385, the expression of GPX4 further decreased compared to the HG group. The results indicate that Sirt6

can have a protective effect on podocytes and inhibit the occurrence of ferroptosis in podocytes through factors such as Nrf2 and its downstream GPX4.

## 4. Discussion

Diabetes, a metabolic disease characterized by hyperglycemia, is experiencing a global increase in incidence [23]. In my country, there are currently 140 million adult patients with diabetes, making it the highest in the world. This number is projected to rise to 174 million by 2045 [24]. Diabetes can lead to various severe macrovascular and microvascular complications, making it a significant public health concern worldwide [25]. DN is a critical microvascular complication associated with diabetes. Recent epidemiological surveys indicate that DN accounts for nearly half of all cases of chronic kidney disease and has emerged as the leading cause of ESRD [26]. In this study, we examined the biochemical indicators of blood and urine in mice from the DN db/db group. We observed that 24-h urine protein and blood creatinine levels increased over time, indicating worsening renal function damage. Compared to the db/m group, the glomeruli and renal tubules of the db/db group showed various pathological changes, including thickening of the glomerular basement membrane, degeneration and atrophy of renal tubular epithelial cells, and increased extracellular matrix. Results from HE, PAS, and Masson staining confirmed severe renal damage in the mice from the db/db group. Podocytes play a crucial role in maintaining the normal

glomerular filtration barrier and preventing podocyte damage. Damage to podocytes leads to impaired glomerular filtration barrier integrity, resulting in proteinuria. Several studies have reported that podocyte injury is an early event in diabetic nephropathy. The extent of podocyte damage can serve as an important indicator for evaluating the prognosis of diabetic nephropathy. However, the underlying regulatory mechanisms of podocyte damage remain unclear [27–29]. Electron microscopy results revealed extensive fusion of foot processes and irregular thickening of the basement membrane, providing evidence that podocyte damage is a significant step in the development of diabetic nephropathy.

Clinical intervention measures for diabetic nephropathy (DN) primarily focus on controlling risk factors such as blood sugar, hypertension, and proteinuria. Recent drug clinical trials have shown promising results in managing DN, including the use of SGLT-2 inhibitors and MRA, which can reduce proteinuria levels and slow down the progression of renal function decline. However, altering the outcome of DN progressing to end-stage renal disease (ESRD) remains challenging. Sirtuins, which are involved in various diseases like diabetes, inflammation, metabolic syndrome, and cancer, have gained significant attention [30]. Among them, Sirt6 has been extensively studied and found to play a protective role in the kidney by reducing early podocyte damage in DN [31]. Sirt6 achieves this by activating M2 macrophages and improving podocyte damage caused by DN [32]. Studies have shown that the expression of Sirt6 is reduced in podocytes of DN patients and the renal cortex of DN mice [15]. The expression level of Sirt6 is positively correlated with the patient's glomerular filtration rate, while the proteinuria level is negatively correlated. In diabetic nephropathy mice, Sirt6 expression is decreased while levels of H3K9, TIMP-1, and TGF-β1 rise, causing proximal tubular damage and worsening renal fibrosis [33]. Overexpressing Sirt6 has been shown to protect the kidney by inhibiting Smad3 [16] acetylation, modulating the Notch pathway, and exerting anti-inflammatory and anti-apoptotic effects, cytoskeletal remodeling, and autophagy promotion, all of which help reduce proteinuria [15]. Our study demonstrates a reduction in the expression of Sirt6 in the renal tissue of diabetic mice and in high-glucose-induced podocyte injury, further confirming the close relationship between Sirt6 and the occurrence and development of DN. SOD2 (Superoxide Dismutase 2) and HO1 (Heme Oxygenase 1) are an essential component of the cellular antioxidant defense system, especially in combating oxidative stress and maintaining cellular homeostasis. Additionally, the reduced expression of oxidative stress indicators HO1 and SOD2 in renal tissue suggests that oxidative stress plays a significant role in the pathogenesis of DN. To investigate the relationship between the expression level of Sirt6 and the duration of high-glucose stimulation, we conducted experiments using a high-glucose-induced podocyte injury model at different time points. We found that the expression of Sirt6 reached its lowest point 48 h after high-glucose stimulation, indicating that the duration of high glucose stimulation may independently contribute to the reduction of Sirt6

expression in glomerular podocytes. Based on this finding, we selected the optimal time point for high glucose stimulation. Immunofluorescence analysis revealed a significant reduction in the expression of Sirt6 in the nucleus, as well as reduced expression of Nrf2, GPX4, HO1, and SOD2. Our study shows reduced Sirt6 protein in podocytes of diabetic db/db mice versus controls (Figure 3E). This finding is consistent with the impaired cellular protective mechanisms observed in diabetic nephropathy. Sirt6 is a multifunctional protein deacetylase that plays a crucial role in maintaining cellular metabolism, antioxidant defense, and cellular aging. The reduction of Sirt6 in podocytes may diminish the resistance of these cells to diabetes-related stress, thereby leading to podocyte injury and dysfunction.

The accumulation of ROS plays a crucial role in triggering ferroptosis, and oxidative stress can enhance cellular ferroptosis through various signaling pathways. Wu et al. discovered that ferroptosis is implicated in the pathological progression of podocyte damage in diabetic nephropathy caused by high fructose intake. They observed a decrease in the expression of ferroptosis marker proteins, SLC7A11 and GPX4, along with an accumulation of lipid peroxides. The administration of ferroptosis inhibitors demonstrated a reduction in podocyte damage [34]. Building on this theoretical foundation, this study further investigated the association between Sirt6 and ferroptosis in diabetic nephropathy.

Ferroptosis, a distinct form of programmed cell death, exhibits notable differences in cell morphology and function compared to apoptosis, autophagy, and necrosis. Key features of ferroptosis include decreased levels of GSH, inhibition of GPX4 activity, accumulation of ROS and lipid peroxidation, ultimately resulting in cell death [35–37]. In a study by Li et al. [38], it was observed that renal tissues and cells of DN mice displayed iron overload, reduced antioxidant capacity, and increased accumulation of ROS along with lipid peroxidation. Furthermore, renal biopsy samples from DN patients exhibited reduced levels of GPX4 protein and mRNA, decreased concentration of GSH, and enhanced lipid peroxidation [39]. Nrf2, a crucial transcription factor responsible for cellular resistance against oxidative damage, also serves as a key regulator of ferroptosis resistance, influencing the expression of GPX4, HO-1, and more [40]. The lack of GPX4 is considered a significant indicator of ferroptosis. In cells and tissues of DN, the expression of GPX4 and SLC7A11 is reduced, leading to a significant increase in ROS levels in the body and the occurrence of ferroptosis [38, 41]. In our study, we used the ferroptosis inhibitor Fer-1 to investigate high glucose-induced podocyte injury. We observed an increase in the expression of Nrf2, SLC7A11, and GPX4, a decrease in the expression of ACSL4, an increase in the levels of GSH and SOD, and a decrease in the level of MDA. In our study, ACSL4 expression was elevated in the high-glucose (HG) group versus the normal-glucose (NG) group, aligning with the heightened ferroptosis and oxidative stress seen in diabetic nephropathy. Given ACSL4's role as a pivotal enzyme in lipid metabolism, this upregulation could foster the synthesis of lipids prone to oxidation, escalating ferroptosis risk. Notably,

HG-treated podocytes exhibited decreased ACSL4 expression upon Fer-1 treatment, implying that Fer-1's protective action on podocytes may stem from its ability to suppress ACSL4 and, consequently, inhibit ferroptosis. This underscores the significance of ferroptosis in podocyte injury within diabetic kidney disease and hints at the multifaceted mechanisms of Fer-1. These findings suggest a close relationship between ferroptosis and the development of DN, and indicate that inhibiting ferroptosis can effectively reduce cellular lipid peroxidation.

Based on the research findings, it has been demonstrated that oxidative stress and ferroptosis play a role in the damage of podocytes and tissues in diabetic nephropathy. Several studies have indicated that the regulation of Sirt6 can offer protection to podocytes and decrease the production of proteinuria through various mechanisms, such as anti-inflammation, anti-apoptosis, involvement in cytoskeletal remodeling, and promotion of autophagy [15]. Furthermore, it has been observed that the knockout of Sirt6 exacerbates renal injury associated with diabetic nephropathy and leads to the development of proteinuria [16, 42]. Nephrin, a key component of the podocyte slit diaphragm, is essential for the glomerular filtration barrier's integrity [43]. Its downregulation often signals the onset of proteinuria and is a hallmark of diabetic nephropathy. Our findings align with prior research, showing that nephrin expression decreases under high-glucose stimulation. Notably, Sirt6 overexpression elevates nephrin levels, suggesting it may protect podocytes against injury induced by high glucose. Nrf2/GPX4 are key factors in oxidative stress and ferroptosis. Li [38] found that upregulating Nrf2 can inhibit changes related to ferroptosis, thereby delaying the progression of diabetic nephropathy. In this study, we investigated the potential protective effect of Sirt6 on ferroptosis in DN and explored its relationship with the Nrf2/GPX4 signaling pathway. To our knowledge, no previous studies have reported on the association between Sirt6 and ferroptosis. Our hypothesis was that by regulating Sirt6, the occurrence of ferroptosis could be alleviated through the Nrf2/GPX4 signaling pathway. To test this hypothesis, we transfected podocytes cultured with high glucose with Sirt6 full-length plasmid, Sirt6 siRNA and the Nrf2/GPX4 pathway was inhibited using the specific inhibitor ML385. Our results showed that by manipulating the expression of Sirt6, the levels of Nrf2, ACSL4, HO1, and GPX4 were also affected. Overexpression of Sirt6 led to improved expression of ferroptosis and oxidative stress biomarkers, increased mitochondrial membrane potential energy, and maintained the integrity of mitochondrial structure, ultimately protecting podocytes. In this experiment, we transfected podocytes with a Sirt6 plasmid to overexpress Sirt6 and introduced the Nrf2-specific inhibitor ML385 to inhibit the Nrf2/GPX4 pathway. In summary, Sirt6 overexpression can mitigate high-glucose-induced oxidative stress and ferroptosis in HPC cells, potentially through modulation of the Nrf2/GPX4 pathway.

Based on our experimental results, we propose several potential mechanisms about Sirt6 in regulating ferroptosis in podocyte injury associated with diabetic nephropathy.

1. Antioxidative stress: Sirt6, a deacetylase, bolsters cellular antioxidant capacity. We observed decreased Sirt6 expression under high-glucose conditions, potentially weakening antioxidant defenses and predisposing cells to ferroptosis. 2. Nrf2/GPX4 pathway regulation: Our results show that Sirt6 overexpression can diminish ferroptosis by activating the Nrf2/GPX4 pathway. Nrf2, a key transcription factor, upregulates antioxidant enzymes like GPX4, which are vital for countering ferroptosis. 3. Mitochondrial function protection: We also found that Sirt6 enhances mitochondrial function and structure—critical sites for oxidative stress and lipid peroxidation in ferroptosis. Overexpression of Sirt6 elevated mitochondrial membrane potential and preserved mitochondrial morphology, possibly reducing ferroptosis.

In conclusion, our study demonstrates the significant involvement of ferroptosis in the onset and progression of diabetic nephropathy. We found that increasing the expression of Sirt6 can mitigate high-glucose-induced ferroptosis and ameliorate mitochondrial morphology and functional impairments. These findings offer a novel approach for the prevention and treatment of diabetic nephropathy.

## Authors' contributions

Lingyu Du, Canghui Guo, Shengnan Zeng, Ke Yu, Maodong Liu and Ying Li conceived and designed the present study. Lingyu Du was responsible for data analysis and performed the experiments. Lingyu Du wrote and edited the manuscript. Ying Li reviewed and edited the manuscript. All authors read and approved the final manuscript.

## Disclosure statement

No potential conflict of interest was reported by the author(s).

## Ethical approval

The animal protocol was reviewed and approved by the Laboratory Animal Ethical and Welfare Committee of Hebei Medical University, approval number (2023019).

## Funding

## Data availability statement

All data generated during the study can be obtained upon reasonable request from the corresponding author.

## References

[1]  Gonzalez CD, Carro Negueruela MP, Nicora Santamarina C, et al. Autophagy dysregulation in diabetic kidney

disease: from pathophysiology to pharmacological interventions. Cells. 2021;10(9):2497. doi:10.3390/cells10092497.

[2] Tuttle KR, Agarwal R, Alpers CE, et al. Molecular mechanisms and therapeutic targets for diabetic kidney disease. Kidney Int. 2022;102(2):248–260. doi:10.1016/j.kint.2022.05.012.

[3] Natesan V, Kim SJ. Diabetic nephropathy – a review of risk factors, progression, mechanism, and dietary management. Biomol Ther (Seoul). 2021;29(4):365–372. doi:10.4062/biomolther.2020.204.

[4] Yang D, Livingston MJ, Liu Z, et al. Autophagy in diabetic kidney disease: regulation, pathological role and therapeutic potential. Cell Mol Life Sci. 2018;75(4):669–688. doi:10.1007/s00018-017-2639-1.

[5] Tang SCW, Yiu WH. Innate immunity in diabetic kidney disease. Nat Rev Nephrol. 2020;16(4):206–222. doi:10.1038/s41581-019-0234-4.

[6] Iatcu CO, Steen A, Covasa M. Gut microbiota and complications of type-2 diabetes. Nutrients. 2021;14(1):166. doi:10.3390/nu14010166.

[7] Jung CY, Yoo TH. Pathophysiologic mechanisms and potential biomarkers in diabetic kidney disease. Diabetes Metab J. 2022;46(2):181–197. doi:10.4093/dmj.2021.0329.

[8] Wang S, Zhang X, Wang Q, et al. Histone modification in podocyte injury of diabetic nephropathy. J Mol Med (Berl). 2022;100(10):1373–1386. doi:10.1007/s00109-022-02247-7.

[9] Watanabe K, et al. What's new in the molecular mechanisms of diabetic kidney disease: recent advances. Int J Mol Sci. 2022;24(1):570. doi:10.3390/ijms24010570.

[10] Chen X, Wang J, Lin Y, et al. Signaling pathways of podocyte injury in diabetic kidney disease and the effect of sodium-glucose cotransporter 2 inhibitors. Cells. 2022;11(23):3913. doi:10.3390/cells11233913.

[11] Bian C, Ren H. Sirtuin family and diabetic kidney disease. Front Endocrinol (Lausanne). 2022;13:901066. doi:10.3389/fendo.2022.901066.

[12] Kuang J, Chen L, Tang Q, et al. The role of Sirt6 in obesity and diabetes. Front Physiol. 2018;9:135. doi:10.3389/fphys.2018.00135.

[13] Yang X, Feng J, Liang W, et al. Roles of SIRT6 in kidney disease: a novel therapeutic target. Cell Mol Life Sci. 2021;79(1):53. doi:10.1007/s00018-021-04061-9.

[14] Fan Y, Yang Q, Yang Y, et al. Sirt6 suppresses high glucose-induced mitochondrial dysfunction and apoptosis in podocytes through AMPK activation. Int J Biol Sci. 2019;15(3):701–713. doi:10.7150/ijbs.29323.

[15] Liu M, Liang K, Zhen J, et al. Sirt6 deficiency exacerbates podocyte injury and proteinuria through targeting Notch signaling. Nat Commun. 2017;8(1):413. doi:10.1038/s41467-017-00498-4.

[16] Wang X, Ji T, Li X, et al. FOXO3a protects against kidney injury in type ii diabetic nephropathy by promoting Sirt6 expression and inhibiting Smad3 acetylation. Oxid Med Cell Longev. 2021;2021:5565761. doi:10.1155/2021/5565761.

[17] Dixon SJ, Lemberg KM, Lamprecht MR, et al. Ferroptosis: an iron-dependent form of nonapoptotic cell death. Cell. 2012;149(5):1060–1072. doi:10.1016/j.cell.2012.03.042.

[18] Li J, Cao F, Yin H-L, et al. Ferroptosis: past, present and future. Cell Death Dis. 2020;11(2):88. doi:10.1038/s41419-020-2298-2.

[19] Jiang X, Stockwell BR, Conrad M. Ferroptosis: mechanisms, biology and role in disease. Nat Rev Mol Cell Biol. 2021;22(4):266–282. doi:10.1038/s41580-020-00324-8.

[20] Wang Y, Wang S, Xin Y, et al. Hydrogen sulfide alleviates the anxiety-like and depressive-like behaviors of type 1 diabetic mice via inhibiting inflammation and ferroptosis. Life Sci. 2021;278:119551. doi:10.1016/j.lfs.2021.119551.

[21] Feng S, Li Y, Huang H, et al. Isoorientin reverses lung cancer drug resistance by promoting ferroptosis via the SIRT6/Nrf2/GPX4 signaling pathway. Eur J Pharmacol. 2023;954:175853. doi:10.1016/j.ejphar.2023.175853.

[22] Mi Y, Wei C, Sun L, et al. Melatonin inhibits ferroptosis and delays age-related cataract by regulating SIRT6/p-Nrf2/GPX4 and SIRT6/NCOA4/FTH1 pathways. Biomed Pharmacother. 2023;157:114048. doi:10.1016/j.biopha.2022.114048.

[23] American Diabetes, A. 2. classification and diagnosis of diabetes: standards of medical care in diabetes-2021. Diabetes Care. 2021;44(Suppl 1):S15–S33. doi:10.2337/dc21-S002.

[24] Sun H, Saeedi P, Karuranga S, et al. IDF diabetes atlas: global, regional and country-level diabetes prevalence estimates for 2021 and projections for 2045. Diabetes Res Clin Pract. 2022;183:109119. doi:10.1016/j.diabres.2021.109119.

[25] Ali MK, Pearson-Stuttard J, Selvin E, et al. Interpreting global trends in type 2 diabetes complications and mortality. Diabetologia. 2022;65(1):3–13. doi:10.1007/s00125-021-05585-2.

[26] Mohandes S, Doke T, Hu H, et al. Molecular pathways that drive diabetic kidney disease. J Clin Invest. 2023;133(4):1–12. doi:10.1172/JCI165654.

[27] Barutta F, Bellini S, Gruden G. Mechanisms of podocyte injury and implications for diabetic nephropathy. Clin Sci (Lond). 2022;136(7):493–520. doi:10.1042/CS20210625.

[28] Fu Y, Sun Y, Wang M, et al. Elevation of JAML promotes diabetic kidney disease by modulating podocyte lipid metabolism. Cell Metab. 2020;32(6):1052–1062 e8. doi:10.1016/j.cmet.2020.10.019.

[29] Li X, Zhang Y, Xing X, et al. Podocyte injury of diabetic nephropathy: novel mechanism discovery and therapeutic prospects. Biomed Pharmacother. 2023;168:115670. doi:10.1016/j.biopha.2023.115670.

[30] Morigi M, Perico L, Benigni A. Sirtuins in renal health and disease. J Am Soc Nephrol. 2018;29(7):1799–1809. doi:10.1681/ASN.2017111218.

[31] Wang Z, Wu Q, Wang H, et al. Diosgenin protects against podocyte injury in early phase of diabetic nephropathy through regulating SIRT6. Phytomedicine. 2022;104:154276. doi:10.1016/j.phymed.2022.154276.

[32] Ji L, Chen Y, Wang H, et al. Overexpression of Sirt6 promotes M2 macrophage transformation, alleviating renal injury in diabetic nephropathy. Int J Oncol. 2019;55(1):103–115. doi:10.3892/ijo.2019.4800.

[33] Muraoka H, Hasegawa K, Sakamaki Y, et al. Role of Nampt-Sirt6 axis in renal proximal tubules in extracellular matrix deposition in diabetic nephropathy. Cell Rep. 2019;27(1):199–212 e5. doi:10.1016/j.celrep.2019.03.024.

[34] Wu W-Y, Wang Z-X, Li T-S, et al. SSBP1 drives high fructose-induced glomerular podocyte ferroptosis via

activating DNA-PK/p53 pathway. Redox Biol. 2022; 52:102303. doi:10.1016/j.redox.2022.102303.

[35] Lv Y, Wu M, Wang Z, et al. Ferroptosis: from regulation of lipid peroxidation to the treatment of diseases. Cell Biol Toxicol. 2023;39(3):827–851. doi:10.1007/s10565-022-09778-2.

[36] Liu J, Kang R, Tang D. Signaling pathways and defense mechanisms of ferroptosis. Febs J. 2022;289(22):7038–7050. doi:10.1111/febs.16059.

[37] Wang Y, Bi R, Quan F, et al. Ferroptosis involves in renal tubular cell death in diabetic nephropathy. Eur J Pharmacol. 2020;888:173574. doi:10.1016/j.ejphar.2020.173574.

[38] Li S, Zheng L, Zhang J, et al. Inhibition of ferroptosis by up-regulating Nrf2 delayed the progression of diabetic nephropathy. Free Radic Biol Med. 2021;162:435–449. doi:10.1016/j.freeradbiomed.2020.10.323.

[39] Kim S, Kang S-W, Joo J, et al. Correction: characterization of ferroptosis in kidney tubular cell death under diabetic conditions. Cell Death Dis. 2021;12(4):382. doi:10.1038/s41419-021-03667-y.

[40] Chen G-H, Song C-C, Pantopoulos K, et al. Mitochondrial oxidative stress mediated Fe-induced ferroptosis via the NRF2-ARE pathway. Free Radic Biol Med. 2022;180:95–107. doi:10.1016/j.freeradbiomed.2022.01.012.

[41] Stockwell BR, Jiang X, Gu W. Emerging mechanisms and disease relevance of ferroptosis. Trends Cell Biol. 2020; 30(6):478–490. doi:10.1016/j.tcb.2020.02.009.

[42] Huang W, L H, Zhu S, et al. Sirt6 deficiency results in progression of glomerular injury in the kidney. Aging (Albany NY). 2017;9(3):1069–1083. doi:10.18632/aging.101214.

[43] Ma S, Qiu Y, Zhang C. Cytoskeleton rearrangement in podocytopathies: an update. Int J Mol Sci. 2024;25(1):25. doi:10.3390/ijms25010647.